Load Transfer Curves along Bored Piles Considering Modulus Degradation

Hong Zhu[1] and Ming-Fang Chang, P.E., M.ASCE[2]

Abstract: The load-transfer (or *t-z*) curve, which reflects the interaction between a pile and the surrounding soil, is important for evaluating the load-settlement response of a pile subjected to an axial load using the load-transfer method. Preferably, the nonlinear stress-strain behavior of the soil should be incorporated into the *t-z* curve. This paper presents a practical approach for the estimation of *t-z* curves along bored piles by considering the nonlinear elastic properties and modulus degradation characteristics of the soil. A method for evaluating the modulus degradation curve from the results of a pressuremeter test is proposed. The results of load tests on one instrumented bored pile in Piedmont residual soil in Atlanta and another in the residual soil of the Jurong Formation in Singapore provide verification of the validity of the proposed approach.

DOI: 10.1061/(ASCE)1090-0241(2002)128:9(764)

CE Database keywords: Load transfer; Bored piles; Degradation; Load tests; Soil-pile interaction; Nonlinear response.

Introduction

The load-transfer method of analysis (Colye and Reese 1966) is widely used for prediction of the load-settlement relationship for piles subject to axial loads because of its simplicity and capability of incorporating nonlinear soil behavior. A load-transfer curve, or *t-z* curve, which describes the relationship between the unit resistance transferred to the surrounding soil and the displacement of the pile relative to the soil in each geological stratum, is required in the analysis. Numerous load-transfer (*t-z*) models or functions have been proposed for the load-transfer analysis of bored piles. These functions generally fall into two main categories: (1) empirical functions (e.g., Colye and Reese 1966; Vijayvergiya 1977; Reese and O'Neill 1988) and (2) theoretical functions (e.g., Randolph and Wroth 1978; Kraft et al. 1981). While the earlier category has its practical value, the latter category is more attractive because of the flexibility with which site specific strength and deformation properties of soils can be readily incorporated.

The stress-strain behavior of natural soils during shear is highly nonlinear and the elastic modulus generally decreases with increase in shear strain. Extensive studies based on both numerical analysis and field monitoring have shown that this degradation of soil shear modulus G with shear strain, or shear stress, significantly influences the performance of a foundation system, especially in stiff soils (e.g., Jardine et al. 1986). Therefore, one needs to consider the strain/stress-level-dependent shear behavior of soils in analyses of the foundation response. This is particularly important when a pile is subjected to axial loading in which the shear strain in the surrounding soil gradually and progressively increases from a small strain to a large strain as the applied load increases. Existing *t-z* functions are either highly empirical or based on oversimplified theoretical frameworks without proper account of the modulus degradation characteristics of soils.

This paper describes a proposed procedure for the evaluation of load-transfer curves along bored piles in residual soils and weathered rocks by considering modulus degradation. An approximate analytical solution presented by Randolph and Wroth (1978) is modified to account for modulus degradation of soils. The modified hyperbolic function proposed by Fahey and Carter (1993) is used for the description of the modulus degradation curves derived from results of pressuremeter tests. Load test data from instrumented bored piles in Piedmont residual soil in Atlanta and the residual soil of the Jurong Formation in Singapore provide a basis for verification of the proposed procedure.

Modulus Degradation

The stress-strain behavior of most geomaterials is highly nonlinear at all phases of loading. A true linear elastic behavior is only observed for soils at a very small strain level and usually there is a marked reduction in stiffness with increasing strain level. An S-shaped degradation curve, as shown schematically in Fig. 1, is commonly found not only in laboratory tests (e.g., Jardine et al. 1986) but also in in situ tests (e.g., Powell and Butcher 1991; Pinto and Abramento 1997).

In order to incorporate the nonlinear feature of stress-strain behavior into numerical analyses, one needs to describe mathematically the modulus degradation curve or the modulus–strain-level relationship. Numerous expressions have been proposed to describe modulus degradation for different soils. Although simple hyperbolas (i.e., Kondner 1963) provide some convenience because only two or three parameters are needed, they are not sufficient for precise description of the generally complicated degradation in most cases. On the other hand, more accurate curve

[1]Geotechnical Engineer, Land Transport Authority, 251 North Bridge Rd., Singapore 179102; formerly, Graduate Student, School of Civil and Environmental Engineering, Nanyang Technological Univ., Block N1, Nanyang Ave., Singapore 639798.

[2]Associate Professor, School of Civil and Environmental Engineering, Nanyang Technological Univ., Block N1, Nanyang Ave., Singapore 639798.

Note. Discussion open until February 1, 2003. Separate discussions must be submitted for individual papers. To extend the closing date by one month, a written request must be filed with the ASCE Managing Editor. The manuscript for this paper was submitted for review and possible publication on March 27, 2001; approved on February 18, 2002. This paper is part of the ***Journal of Geotechnical and Geoenvironmental Engineering***, Vol. 128, No. 9, September 1, 2002. ©ASCE, ISSN 1090-0241/2002/9-764–774/$8.00+$.50 per page.

J. Geotech. Geoenviron. Eng. 2002.128:764-774.

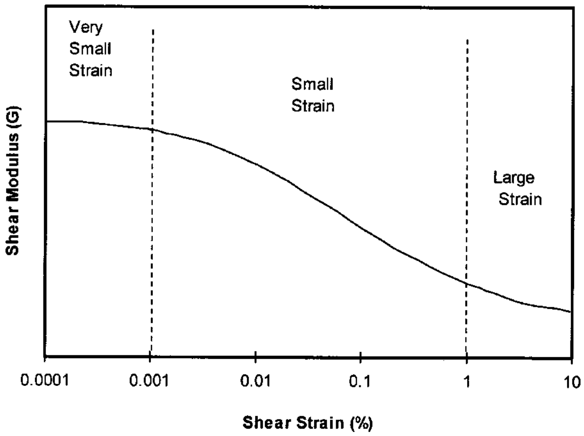

Fig. 1. Characteristic ranges of stiffness of soils

fitting procedures often result in highly sophisticated functions. For example, a periodic logarithmic function as proposed by Jardine et al. (1986) requires five parameters. The modified hyperbolic expression proposed by Fahey and Carter (1993) appears to be advantageous over others because fewer parameters are involved and it has a more flexible curve shape. The expression takes the following form:

$$\frac{G}{G_{\max}}=1-f\cdot\left(\frac{\tau}{\tau_{\max}}\right)^{g} \tag{1}$$

where $G, G_{\max}$=current and maximum shear modulus of the soil, respectively; $\tau, \tau_{\max}$=current and maximum shear stress, respectively; and f and g=curve fitting parameters.

Fig. 2(a) shows sample shear modulus degradation curves,

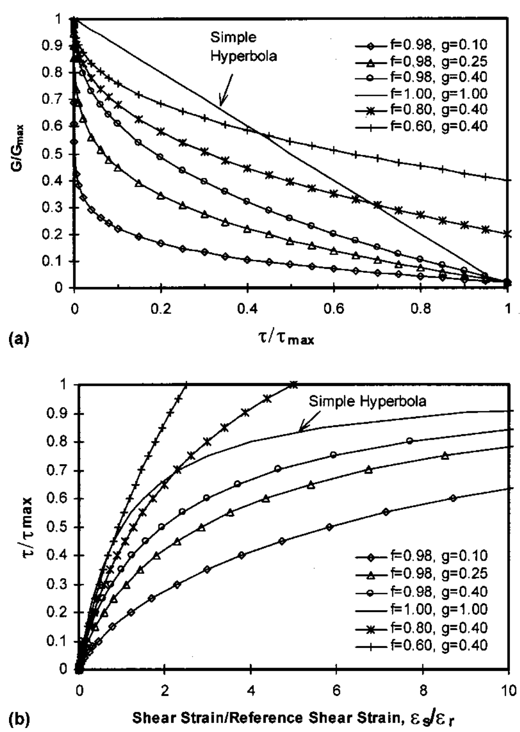

Fig. 2. Effect of stress or strain level on shear modulus: (a) theoretical modulus degradation curves; (b) theoretical stress-strain curves

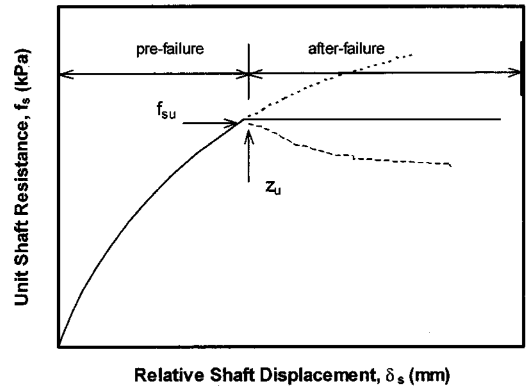

Fig. 3. Schematic presentation of proposed *t-z* curve

presented as the variation of the normalized shear modulus $G/G_{\max}$ with the shear stress level $\tau/\tau_{\max}$, generated by Eq. (1). The parameter f controls the magnitude or the extent of degradation whereas the parameter g dictates the rate of degradation and the curvature of the curve. Fig. 2(b) shows the normalized stress-strain curves corresponding to the modulus degradation curves in Fig. 2(a), where the reference shear strain ε_r is defined as $\tau_{\max}/G_{\max}$. It is noted that an increasing g value corresponds to a stiffer and stronger soil, but an increasing f value corresponds to a weaker and less rigid soil. The parameter f resembles the failure ratio R_f that is commonly used in describing the stress-strain curve in a conventional hyperbolic model.

Proposed Theoretical *t-z* Curve

The proposed load transfer (*t-z*) curve, as shown in Fig. 3, consists of two parts: (1) a modified hyperbolic prefailure portion and (2) a perfectly plastic after-failure portion. The soil around a pile is assumed to deform in a simple shear mode before the unit shaft resistance (f_s) reaches its ultimate value (f_{su}). A discontinuous failure surface may be generated within the soil immediately next to the pile or at the soil-pile interface when the relative shaft displacement exceeds the critical shaft displacement z_u and the mobilized shaft resistance reaches the f_{su} value. Different shear mechanisms require the employment of different methods of construction for the prefailure and the after-failure portions of a *t-z* curve. These methods are discussed in the following subsections in detail. Postpeak softening or hardening behavior of the soil, as illustrated in Fig. 3, is not considered.

Evaluation of Prefailure t-z Curve

The prediction of the prefailure portion of the *t-z* curve is based on an approximate analytical solution presented by Randolph and Wroth (1978) for analysis of the settlement of a single pile. The displacement of a shaft element z_s is related to the local shaft stress τ_0 and the shear modulus of the soil mass G. For piles with slenderness ratio L/r_0 of 20 or more, z_s can be approximately expressed by

$$z_s \cong \tau_0 r_0 \int_{r_0}^{\infty} \frac{dr}{Gr} \tag{2}$$

in which r_0=radius of the shaft. It is noted from Eq. (2) that z_s diverges as the radial distance from the pile increases. To extract a bounded solution from this unbounded condition, Randolph and

J. Geotech. Geoenviron. Eng. 2002.128:764-774.

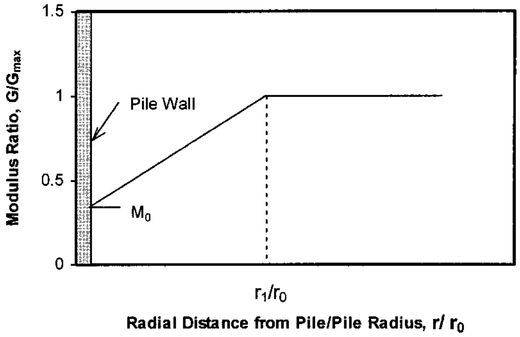

Fig. 4. Idealized radial distribution of soil modulus ratio (after Kraft et al. 1981)

Wroth (1978) introduced a limiting radius r_m at which the shear stress becomes negligible. Randolph and Wroth (1978) found that the value of r_m varies with depth, and its suitable average value within the entire pile length for a homogeneous soil profile can be expressed in terms of the pile length L as

$$r_m = 2.5L(1-\nu_s) \tag{3}$$

where ν_s = Poisson's ratio of soil.

By introducing Eq. (1) into Eq. (2) and integrating, Eq. (2) becomes (Chang and Zhu 1998)

$$z_s = \frac{\tau_0 r_0}{G_{\max} g} \ln\left[\frac{\left(\frac{r_m}{r_0}\right)^g - f\left(\frac{\tau_0}{\tau_{\max}}\right)^g}{1-f\left(\frac{\tau_0}{\tau_{\max}}\right)^g}\right] \tag{4}$$

If g and f are set to 1 and R_f, respectively, the above equation is then simplified to

$$z_s = \frac{\tau_0 r_0}{G_{\max}} \ln\left[\frac{\left(\frac{r_m}{r_0}\right) - R_f\left(\frac{\tau_0}{\tau_{\max}}\right)}{1-R_f\left(\frac{\tau_0}{\tau_{\max}}\right)}\right] \tag{5}$$

which is identical to the expression developed by Kraft et al. (1981) using a conventional hyperbolic soil model.

Eq. (4) can be used to generate a series of prefailure *t-z* curves, by varying the soil parameters for a pile that is embedded in a homogeneous soil. However, in practice, the stiffness of natural soils generally increases with depth and there may exist a softened annular zone of material around the pile shaft for bored piles. As such, soil inhomogeneity will need to be considered in order to enhance the versatility of the formulation.

Variation of Shear Modulus with Radial Distance

If the soil modulus is assumed to be proportional to the shear strength of the soil, then the deduced modulus next to the pile can be estimated from the shear strength of the soil after installation and prior to loading. Since the actual distribution of shear strength is not known with a reasonable precision, an idealized linear distribution, with $G/G_{\max}$ equal to M_0 at the pile-soil interface and increasing linearly to a value of 1.0 at the elastic-plastic boundary r_1, as suggested by Kraft et al. (1981), may be used. The resulting normalized shear modulus versus normalized radial distance from the pile/soil interface is as shown in Fig. 4. The average soil modulus in this case is (Kraft et al. 1981)

$$G_{\text{ave}} = G_{\max} \frac{\ln\left(\frac{r_m}{r_0}\right)}{\frac{\left(\frac{r_1}{r_0}\right)-1}{\left(\frac{M_0 r_1}{r_0}\right)-1}\ln\left(\frac{M_0 r_1}{r_0}\right) + \ln\left(\frac{r_m}{r_1}\right)} \tag{6}$$

in which G_{ave} = equivalent shear modulus for the soil-pile system; and r_1 and M_0 are as defined in Fig. 4. From numerical analyses, Zhu (2000) found that the r_1/r_0 value is in the range of 6–8 for stiff clayey soils. Field measurements gathered at Houston University in Houston showed that this value could be 2–3 for heavily overconsolidated clay (O'Neill 2001).

Variation of Shear Modulus with Depth

The soil shear modulus distribution along a pile can be described as a power function of depth as follows:

$$G = A_g z^n \tag{7}$$

where A_g and n are constants; and z = depth below the ground surface (Guo and Randolph 1997). By adopting various combinations of values for A_g and n, Eq. (7) is able to describe different patterns of the variation of soil modulus with depth, such as constant, linearly or nonlinearly increasing with depth, or linearly or nonlinearly decreasing with depth. The average shear modulus along a pile with an embedment length L can then be estimated as

$$G_{\text{ave}} = A_g L^n/(n+1) \tag{8}$$

To account for the influence of vertical inhomogeneity on the maximum radius of influence r_m, Randolph and Wroth (1978) introduced an inhomogeneity factor ρ, which is the ratio of the shear modulus at the middepth below the pile head to that at the base, into Eq. (3). The new expression for r_m is

$$r_m = 2.5L\rho(1-\nu_s) \tag{9}$$

In a generalized form, r_m can be expressed as (Guo and Randolph 1997)

$$r_m = A\frac{1-\nu_s}{1+n}L + Br_0 \tag{10}$$

where A,B are factors depending on the pile geometry, pile-soil stiffness, and soil inhomogeneity.

Evaluation of Ultimate Unit Shaft Resistance

Two approaches, one analytical and the other empirical, are usually used to determine the ultimate unit shaft resistance f_{su}. In the analytical approach, f_{su} is determined based on a static formula using soil parameters derived from both laboratory and in situ tests, whereas, in the empirical approach, f_{su} is directly correlated with results of in situ tests in soils.

Analytical Approach

The effective stress method is employed to calculate f_{su} in the drained condition. The following equation modified from that proposed by Kulhawy (1991) can be adopted:

$$f_{su} = f_K K_0 \sigma'_{v0} \tan\delta' = K\sigma'_{v0}\tan\delta' \tag{11}$$

where f_k = factor reflecting the construction effect on the horizontal stress; K_0 = coefficient of earth pressure at rest; σ'_{v0} = initial effective vertical stress of soil; δ' = effective friction angle for the soil-pile interface; and K = coefficient of earth pressure after pile

J. Geotech. Geoenviron. Eng. 2002.128:764-774.

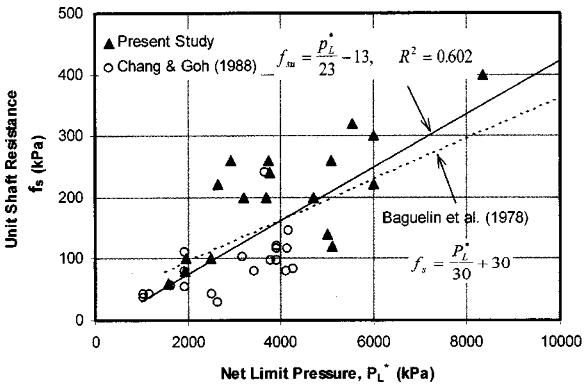

Fig. 5. Relationship between f_{su} and p_L^* for residual soils of Singapore (after Zhu 2000)

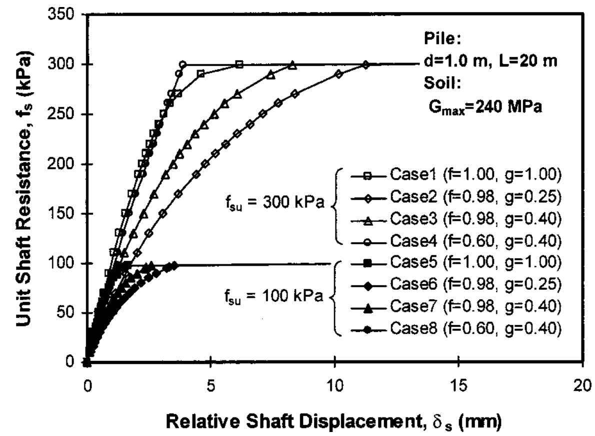

Fig. 6. Effect of factors f and g and ultimate skin friction of *t-z* curves

installation. The parameter f_k is related to K_0; its value is a function of the concrete pressure and the construction method, as well as the influence of both factors on the in situ stress, according to Kulhawy (1991).

Empirical Approach

Numerous empirical correlations between f_{su} and relevant soil parameters from in situ tests are presently available (e.g., Meyerhof 1956; Baguelin et al. 1978). For instance, based on the penetration resistance or N value (in blows/0.3 m) from the standard penetration test, Chang and Broms (1991) proposed the following relationship for the valuation of f_{su} in the design of bored piles in the residual soil of Singapore:

$$f_{su} = 2N \quad (\text{kPa}) \tag{12}$$

The net limit pressure p_L^* from pressuremeter tests is another soil parameter commonly correlated with f_{su}. For instance, Baguelin et al. (1978) proposed a graph for estimating f_{su} for piles in soils with $p_L^* < 1{,}500$ kPa. They suggested that $f_{su} = p_L^*/30 + 30$ can be used for piles in soils with $p_L^* > 1{,}500$ kPa. Fig. 5 shows a similar relationship between p_L^* and f_{su} for bored piles in the residual soil of Singapore based on data collected by Chang and Goh (1988) and Zhu (2000). The large scatter arises mainly from the heterogeneous nature of the residual soil in Singapore. The general relationship between p_L^* and f_{su} is as follows:

$$f_{su} = \frac{p_L^*}{23} - 13 \tag{13}$$

Parametric Study

A parametric study was carried out to examine the effects of the modulus degradation factors (f and g) and the unit shaft resistance (f_{su}) on the *t-z* curve. A bored pile with a diameter of 1.0 m and a length of 20 m was selected for the study. The maximum shear modulus of surrounding soil was assumed to be 240 MPa. Fig. 6 shows the generalized *t-z* curves using four sets of f and g as adopted in Fig. 2. For each set of f and g, two different values of ultimate skin friction, 100 and 300 kPa, were adopted to produce these curves. It is obvious that both the f and g values and the selected f_{su} value have a remarkable effect on the *t-z* curve. A weak soil will have a gentle prefailure curve and a large shaft displacement prior to the full mobilization of the resistance. The effect of f and g becomes less significant when the ultimate skin friction is small.

Determination of Modulus Degradation Curves

The shear modulus degradation curve can be either back-calculated from measured foundation performance data or from direct measurements in the laboratory or form in situ tests.

Back-Calculation from Pile Load Test Results

The principle of this approach is based on the understanding that the foundation performance in response to an applied load is evidently controlled by the behavior of the surrounding soil as it is progressively stressed from a small strain (less than 1%) to a large strain (greater than 1%) as the load increases. Solutions based on elastic theory are usually employed. One such method was described by Mayne (1995).

The elastic theory solution for the vertical displacement δ of a pile subjected to axial compression loading is expressed as (Poulos and Davis 1980)

$$\delta = \frac{QI_\rho}{E_{sL}d} \tag{14}$$

where Q = applied axial load; I_ρ = influence factor; E_{sL} = soil modulus at the shaft base; and d = diameter of the shaft. The factor I_ρ can be determined either by available chart solutions (Poulos and Davis 1980) or by an approximate closed-form solution (Randolph and Wroth 1978, 1979), which is expressed as

$$I_\rho = 4(1+\nu_s)\frac{\left[1 + \frac{1}{\pi\lambda}\frac{8}{(1-\nu_s)}\frac{\eta}{\xi}\frac{\tanh(\mu L)}{\mu L}\frac{L}{d}\right]}{\left[\frac{4}{(1-\nu_s)}\frac{\eta}{\xi} + \frac{4\pi\rho}{\varsigma}\frac{\tanh(\mu L)}{\mu L}\frac{L}{d}\right]} \tag{15}$$

where L = pile length; $\eta = d_b/d$ (d_b = diameter of the base); $\xi = E_{sL}/E_b$ (E_b = soil modulus below foundation base, $E_b = E_{sL}$ for a floating pile); $\rho = E_{sm}/E_{sL}$ (E_{sm} = soil modulus at middepth of pile); $\lambda = 2(1+\nu_s)E_p/E_{sL}$; $\zeta = \ln(\{0.25 + [2.5\rho(1-\nu_s) - 0.25]\xi\}(2L/d))$; $\mu L = 2(2/\zeta\lambda)^{0.5}(L/d)$; and E_p = pile modulus.

The solution given by Eq. (15) can accommodate soil models with a modulus that is either constant or varying linearly with depth (e.g., Guo and Randolph 1997). The modified form of Eq. (14) that accounts for modulus degradation for soil along a pile is

$$\delta = \frac{QI_\rho}{2(1+\nu_s)G_{\max}\left[1 - f\left(\frac{Q}{Q_{\text{ult}}}\right)^g\right]d} \tag{16}$$

J. Geotech. Geoenviron. Eng. 2002.128:764-774.

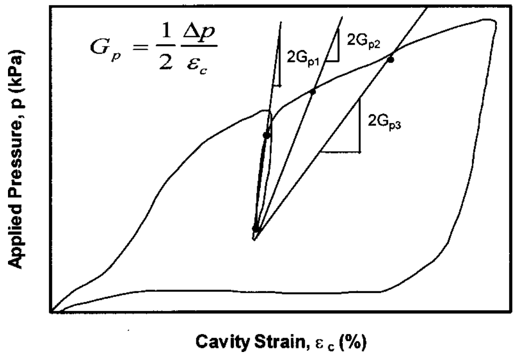

Fig. 7. Deduction of modulus from pressuremeter expansion curve

It is assumed that the ratio of τ/τ_{max} can be considered as the inverse of the factor of safety Q_{ult}/Q, where Q_{ult} is the ultimate axial load resistance of the pile (Mayne 1995).

Direct Measurements

A direct measurement of modulus degradation can be made either in the laboratory or in the field. In the laboratory, results from ultrasonic experiments with torsion shear and the resonant column test combined with those from the triaxial compression test can be utilized to investigate G/G_{max} degradation. In the field, an effective approach for evaluating G/G_{max} degradation involves a combined use of the in situ crosshole test or the in situ spectral analysis of surface waves with the self-boring pressuremeter test or the prebored pressuremeter test (PMT) (Powell and Butcher 1991; Ghionna et al. 1994). In this study, a technique to determine the degradation curve using results from the PMT, one of the most suitable methods of site investigation for residual soils and weathered rocks (Chang 1988), is proposed.

In the pressuremeter test, the pressuremeter shear modulus G_p is usually interpreted as the slope of the selected chord on the observed expansion curve. The relevant expression is (Mair and Wood 1987)

$$G_p = \frac{1}{2}\frac{\Delta p}{\varepsilon_c} \tag{17}$$

where $\Delta p, \varepsilon_c$ = changes in cavity pressure and cavity strain, respectively. The modulus is calculated either from the start of the "true" expansion or from the start of a reloading process. By repeating the above process along the entire expansion curve, the variation of G_p with ε_c can be established. Fig. 7 schematically demonstrates the deduction process in which G_p is calculated from the start of a reloading curve. However, the pressuremeter modulus is not a secant or tangent modulus that can be applied directly in practice. Attempts to link the pressuremeter modulus G_p to the secant shear modulus G_s have been made (e.g., Jardine 1991). A transformed-strain approach as described by Jardine (1991) can be employed to transform an undrained $G_p - \varepsilon_c$ curve into an equivalent undrained $G_s - \varepsilon_s$ (ε_s = shear strain) curve. The process involves simply converting ε_c data points to ε_s data points using the following expression:

$$\frac{\varepsilon_c}{\varepsilon_s} = 1.2 + 0.8\log_{10}\frac{\varepsilon_c}{10^{-5}} \tag{18}$$

The above relationship was established by identifying over the full range of ε_s the value of ε_c at which G_p and G_s are equal.

Evaluation of Soil Parameters

Eqs. (4) and (11) show that the proposed *t-z* curve is a function of the soil stiffness and the interface shear strength. The required soil parameters include the small strain modulus (G_{max}), fitting factors (f,g), the initial coefficient of earth pressure at rest (K_0), the factor of construction effect on the lateral stress (f_k), the effective friction angle at the soil-shaft interface (δ'), and Poisson's ratio of the soil (ν_s). The methodology to determine these parameters is briefly described in the subsequent sections.

Small Strain Modulus G_{max}

The determination of the small strain modulus often requires dynamic tests. Attempts to link G_{max} to conventional soil parameters that can be derived from common in situ tests have been made by various researchers (e.g., Jamiolkowski et al. 1985; Ghionna et al. 1994). For instance, Ghionna et al. (1994) reported that the ratio of G_{max} to the unload-reload pressuremeter modulus G_{ur} was in the range of 1.67–2.38 for Po River sand and Pinto and Abramento (1997) reported a range of 2.10–2.36 for gneissic residual soil in São Paulo, Brazil. An investigation on the basis of ultrasonic velocity measurements, triaxial compression tests with small strain measurements, and OYO pressuremeter tests using the OYO type pressuremeter, carried out as part of this study, shows an average G_{max}/G_{ur} value of 3.0 and a range from 2.5 to 3.5 for the residual soil of the sedimentary Jurong Formation in Singapore.

Fitting Factors f and g

In Eq. (1), G/G_{max} can be alternatively related to the shear strain ε_s as follows:

$$\frac{G}{G_{max}} = 1 - f\cdot\left(\frac{G}{G_{max}}\frac{\varepsilon_s}{\varepsilon_r}\right)^g \tag{19}$$

where $\varepsilon_r = \tau_{max}/G_{max}$ is the reference shear strain.

After the soil modulus versus shear strain is obtained from the pressuremeter expansion curve by the method described in the preceding section, a curve fitting process is carried out subsequently using Eq. (19) to match the data points by varying the values of f and g. The shear strength τ_{max} required can be evaluated from the PMT (Mair and Wood 1987). Chang (1988) proposed the following relationship for evaluating the undrained shear strength of residual soils in Singapore:

$$\tau_{max} = \frac{p_L^*}{12.5} \tag{20}$$

where p_L^* = net limit pressure from the pressuremeter test.

Coefficient of Earth Pressure at Rest K_0

The coefficient of earth pressure at rest K_0 can be either evaluated from in situ tests using the pressuremeter or the dilatometer or estimated from the stress history of the soil. Mayne and Kulhawy (1982) proposed the following equation for estimating the K_0 value from the overconsolidated ratio (OCR) and the effective frictional angle (ϕ') of the soil:

$$K_0 = (1 - \sin\phi')\mathrm{OCR}^{\sin\phi'} \tag{21}$$

J. Geotech. Geoenviron. Eng. 2002.128:764-774.

Table 1. Recommended Interface Friction Angle (Kulhawy 1984)

Pile material	δ'
Rough concrete	ϕ'
Smooth concrete	$0.8\phi'$ to ϕ'
Steel	$0.5\phi'$ to $0.9\phi'$
Timber	$0.8\phi'$ to $0.9\phi'$

Construction Factor f_k

The parameter f_k is related to K_0 and the pile construction method. Withiam and Kulhawy (1981) suggested the following equation for estimation of f_k for bored piles:

$$f_k = \frac{1}{2K_0}\left(K_0 - K_a + (1 - \sin\phi') + \frac{\gamma_c}{\gamma_s}\right) \tag{22}$$

where γ_s, γ_c = bulk unit weights of soil and concrete, respectively; and K_a = Rankine active earth pressure coefficient. Kulhawy (1991) reported that the value of f_k typically varies between 2/3 and 1.

Based on an extensive numerical study, Zhu (2000) found that the combined effects of K_0, type of borehole support, and magnitude of concrete pressure predominantly determined the value of f_k. The factor f_k was also found to vary within the pile length due to nonlinear distribution of concrete pressure (i.e., Construction Industry Research and Information Association 1985; Lings et al. 1994). The effect can be approximately quantified using a dimensionless factor, named the excavation stress ratio ESR, as follows (de Moor 1994):

$$\text{ESR} = \frac{(\sigma_{\text{cont}} - p_b)}{(\sigma_{h0} - p_b)} \tag{23}$$

where σ_{cont} = contact total stress between concrete and borehole wall; σ_{h0} = initial total horizontal stress of soil; and p_b = borehole support pressure. Zhu (2000), by relating the ESR to f_k, proposed an empirical equation that allows one to estimate the f_k at any location along the shaft for any combination of the initial horizontal stress, concrete pressure, and borehole support. The equation is as follows:

$$f_k = 0.29 + 0.68\text{ESR} \tag{24}$$

From Eq. (24), it is clear that the horizontal stress around the shaft after construction may return to its original value only if the concrete pressure reaches the value of the initial horizontal stress; that is, when ESR = 1. However, for stiff clay such as the residual soil, the K_0 value is likely to be larger than 1, and consequently the ESR value is usually less than 1. As a result, it is very unlikely that after construction the horizontal stress in the residual soil around the shaft will recover to its initial value.

Interface Friction Angle δ'

The interface friction angle δ' can be expressed as a function of the internal friction angle ϕ' of the soil. Table 1 shows the value of δ' in relation to ϕ' of the surrounding soil for different interface conditions, as recommended by Kulhawy (1984). Generally, the ϕ' for clays can be measured in the laboratory or estimated from the plasticity index using an empirical relationship, such as that shown in Fig. 8 for the residual soil of the Jurong Formation in Singapore. In the selection of ϕ', a possible deterioration of ϕ' due to the construction effect should be considered. Extensive laboratory and field test results conducted in the residual soil of the Jurong Formation in Singapore (Zhu 2000) revealed that the soaking process, which is one of the major construction factors, could lead to a reduction in the ϕ' value of up to 20% [see also Rahardjo et al. (1995) and Yong et al. (1985)].

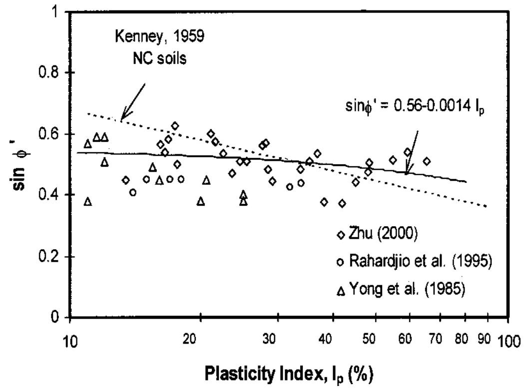

Fig. 8. Relationship between $\sin\phi'$ and plasticity index for residual soil of Jurong Formation

Poisson's Ratio ν_s

The Poisson's ratio, if not directly measured, can be estimated from empirical relationships. For clays, Poulos and Davis's (1980) recommended ranges of values based on soil consistency are 0.3–0.4 for soft clay, 0.2–0.3 for medium stiff clay, and 0.1–0.2 for stiff overconsolidated clay.

Load-Transfer Curve for Pile Tip

Due to difficulty in complete cleaning of the base of a borehole in bored pile construction, a large tip displacement is usually required for the tip resistance to mobilize fully unless the pile is short and rests directly on rocks. Generally, for piles in residual soils with a slenderness ratio of greater than 20, the mobilized tip resistance at the design load may represent a small percentage of the limit tip resistance, with the corresponding degree of mobilization typically less than 20% at twice the design load. It is expected that any minor error in the modeling of the normalized load-transfer curve will not dramatically affect the predicted load-displacement curve until the applied load has exceeded twice the design load.

Chang and Broms (1991) adopted Vijayvergiya's (1977) relationship in order to facilitate the estimation of the load-transfer relationship at the tip for bored piles in residual soils of Singapore. Recommendations were also made on the selection of the limiting tip resistance (q_t) and the critical tip displacement (z_{tc}). Recently, Zhu (2000) analyzed five sets of load-transfer data from bored piles that experienced significant tip displacements (19–33 mm) during load tests in Singapore. The mobilized tip resistance, normalized by the tip resistance q_t^* that corresponds to the maximum pile tip displacement z_t^*, versus the tip displacement, normalized by z_t^*, is shown in Fig. 9. The linear relationship between z_t/z_t^* and q_t/q_t^* indicates that the tip transfer behavior up to twice the design load is essentially linearly elastic and can be simply modeled by the following linear relationship:

$$q_t = k_t z_t \tag{25}$$

where k_t = tip stiffness. For the field data collected in Zhu's (2000) study, k_t is in the range of 95–180 MN/m^3 for the residual soil with a standard penetration resistance (N value) of 150–200 blows/0.3 m.

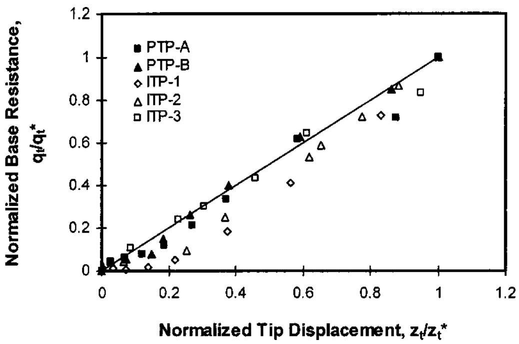

Fig. 9. Normalized load-transfer curve for pile tip

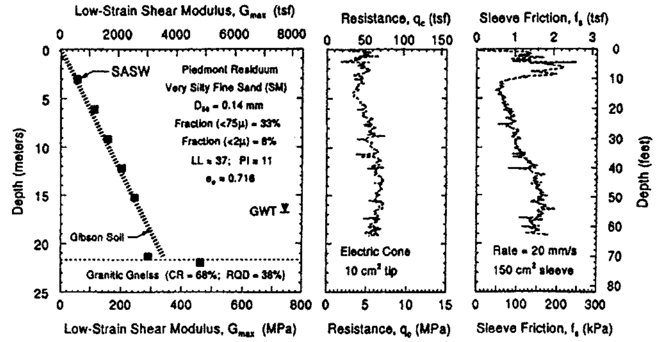

Fig. 11. Profiles of $G_{\max}$, q_c, and f_s at Piedmont test pile site (after Mayne 1995)

Verification of Proposed Approach

In order to examine the validity of the proposed procedure for estimating the load-transfer curves directly or indirectly, two instrumented bored piles were analyzed and their results reviewed. The required input parameters for the analysis, if not provided in the case records, were determined using the procedure outlined in the preceding sections. An analysis was carried out using the program *AXCOL* (Coyle and Reese 1966) for the first pile. The deduced load-displacement curve and load-distribution curves for this pile were then compared with the measurements in the load test to indirectly verify the validity of the proposed approach. For the second pile, a direct comparison was made between the computed and the field back-calculated *t-z* curves. Details of each case study are described in the subsequent sections.

Case 1: Pile in Piedmont Formation, Atlanta

Harris and Mayne (1994) presented the results of axial compression tests on two bored piles installed in Piedmont residual soil on the Georgia Institute of Technology campus in Atlanta. The soils are primarily the product of the in-place weathering of schists, gneisses, and granites. The site was mantled by 1.6 m of fill followed by 16.9 m of residual silty sand overlying partially weathered rock as shown in Fig. 10. The bulk unit weights of the fill and the residual silty sand were both assumed to be 21 kN/m^3. The water table was located at 17.0 m below the ground surface. A "floating" pile with a diameter of 0.76 m and a length of 16.8 m was selected for analysis. Vibrating wire strain gauges were welded to the pile's reinforcing steel at 9.1 and 16.8 m below the ground surface for the pile. The pile modulus (E_p) was assumed to be 20 GPa, as reported by Harris and Mayne (1994).

The site was investigated by in situ tests including the cone penetration test, the dilatometer test, and the spectral analysis of surface waves, among others, and the results are as shown in Fig. 11. The simple Gibson model with the modulus value increasing linearly with depth reasonably describes the $G_{\max}$ profile at the site. Consolidated undrained triaxial compression tests performed on specimens from a range of depths show that the magnitudes of c' and ϕ' within the pile length were relatively constant and were equal to 0 and 36.1°, respectively. The K_0 value can be computed from Eq. (21). Based on the dilatometer test data reported by Harris and Mayne (1994), the average OCR value within the top 7.5 m soil was estimated to be 3, and the value decreased to 1.5 for the soil layer from 7.5 to 16.8 m. Using these OCR values, the corresponding values of K_0 were 0.78 and 0.53, respectively, for the two distinctive soil strata.

Adopting the soil-pile continuum model described earlier and using $\nu_s=0.15$, Mayne (1995) reported that a modified hyperbola with $f=1$ and $g=0.3$ showed a reasonable fit with the backfigured modulus degradation for Piedmont residual soil at the test site. Using the soil properties and key load-transfer parameters listed in Table 2 and the proposed Eq. (4), load-transfer curves can be readily generated for every 1 m section along the pile shaft.

Fig. 12 shows a comparison of the load-displacement curve predicted by integrating the load-transfer curves generated using Eq. (4) along the pile shaft using *AXCOL* and that measured in the load test for the Piedment pile. A good agreement is obtained

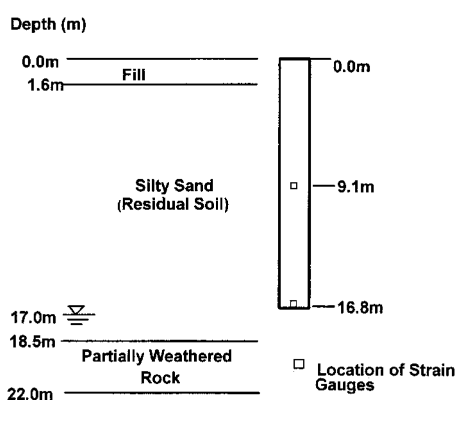

Fig. 10. Soil profile at Piedmont pile location and pile instrumentation

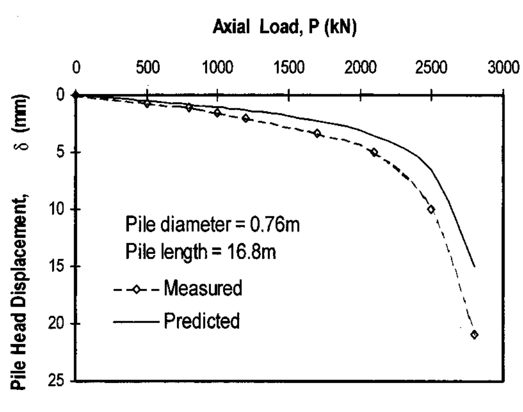

Fig. 12. Predicted and measured load-displacement curve for Piedmont pile

J. Geotech. Geoenviron. Eng. 2002.128:764-774.

Table 2. Soil Properties and Key Load Transfer Parameters along Piedmont Drilled Shaft

Midelement depth (m)	Element length (m)	K_0	σ'_{v0} (kPa)	σ'_{h0} (kPa)	τ_{max} (kPa)	G_{max} (MPa)
0.5	0.5	0.78	11	8.56	5.92	7
1.5	1.0	0.78	33	25.74	17.76	21
2.5	1.0	0.78	55	42.90	29.61	36
3.5	1.0	0.78	77	60.06	41.45	50
4.5	1.0	0.78	99	77.22	53.30	64
5.5	1.0	0.78	121	94.38	65.14	78
6.5	1.0	0.78	143	111.54	76.98	93
7.5	1.0	0.78	165	128.70	88.83	107
8.5	1.0	0.52	187	97.24	65.23	121
9.5	1.0	0.52	209	108.68	73.35	136
10.5	1.0	0.52	231	120.12	81.47	150
11.5	1.0	0.52	253	131.56	89.58	164
12.5	1.0	0.52	275	143.00	97.70	178
13.5	1.0	0.52	297	154.44	105.82	193
14.5	1.0	0.52	319	165.88	113.94	207
15.5	1.0	0.52	341	177.32	122.06	221
16.5	1.0	0.52	363	188.76	130.17	236

Note; $\gamma_t = 21$ kN/m^3; $\phi' = 36.1°$; $f_k = 1.0$; $\delta' = \phi'$.

between the two curves even though some of the soil properties were measured indirectly. Fig. 13 shows the measured axial load distribution compared with the predicted load-distribution curves. A good agreement between the predicted and measured distribution curves is evident. Indirectly the validity of the proposed *t-z* model in Eq. (4) is verified.

Case 2: Pile in Jurong Formation, Singapore

The piling site is located in the south part of Singapore Island. The project involved the construction of an elevated deck in conjunction with the upgrading of a major road to a semiexpressway. Based on the information gathered from the site investigation work and the field boring log, the site is overlaid by a 0.5 m thick layer of soft to stiff, dark grayish clayey silt. From 0.5 to 8.0 m depths, a layer of very hard dark brown and grayish clayey silt (or decomposed siltstone), which is underlaid by a layer of moderately weathered siltstone with a thickness of over 10 m, is present at the site. A preliminary test pile with a diameter of 1.0 m and a penetration depth of 12.0 m, fully instrumented with strain gauges, was constructed. The subsurface ground conditions and the arrangement of instruments for the pile are presented in Fig. 14.

Two OYO type pressuremeter tests were carried out at depths of 2.8 and 4.5 m in a borehole about 5 m away from the test pile prior to the pile construction. In each of the tests, two unload-reload loops were incorporated. Fig. 15 shows the pressuremeter expansion curve for the test at the depth of 2.8 m. The degradation curves of the deduced shear modulus using the procedure illustrated earlier are presented in Fig. 16 along with the best fitting curves. The matching values of f and g are found to be (0.98,0.45) and (0.98,0.25), respectively, as indicated in the figure for PMTs at 2.8 and 4.5 m depths. The measured net limit pressures p_L^* are 7 and 6 MPa, respectively, at the two different depths. The corresponding f_{su} values estimated using Eq. (13) are 291 and 248 kPa, respectively.

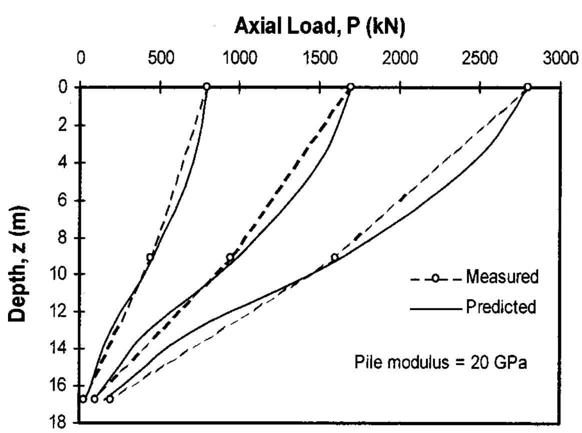

Fig. 13. Predicted and measured distributions of axial load along Piedmont pile

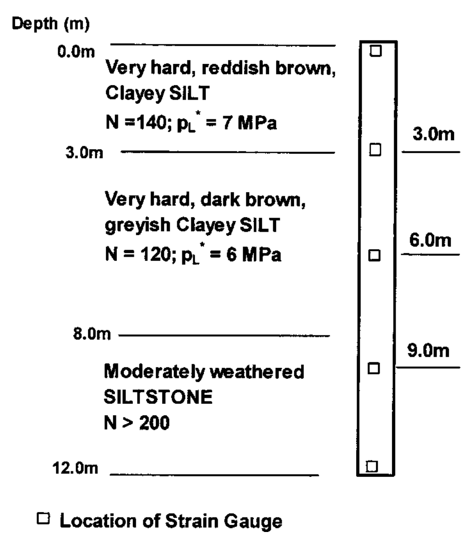

Fig. 14. Soil profile at Singapore test pile site and pile instrumentation

J. Geotech. Geoenviron. Eng. 2002.128:764-774.

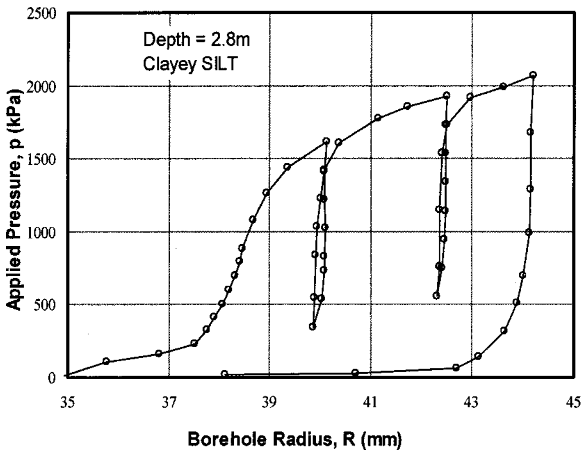

Fig. 15. Pressuremeter expansion curve at 2.8 m depth at Singapore test pile site

As mentioned in the preceding section, the ratio of $G_{\max}$ to G_{ur} for the sedimentary Jurong Formation ranges from 2.5 to 3.5. By adopting a $G_{\max}/G_{ur}$ value of 3.0, the estimated magnitudes of $G_{\max}$ from these two pressuremeter tests are 230 and 200 MPa, respectively, which are similar to those measured by seismic cone penetration tests carried out at the site.

The *t-z* curves predicted for the soil layers 0–3.0 and 3.0–6.0 m using the procedure described earlier and the PMT deduced modulus degradation curves from PMTs at 2.8 and 4.5 m depths are shown in Fig. 17 together with the field deduced load-transfer data and selected reference solutions. There is good agreement between the predicted load-transfer curves and the field observations. The superiority of the present prediction in comparison with

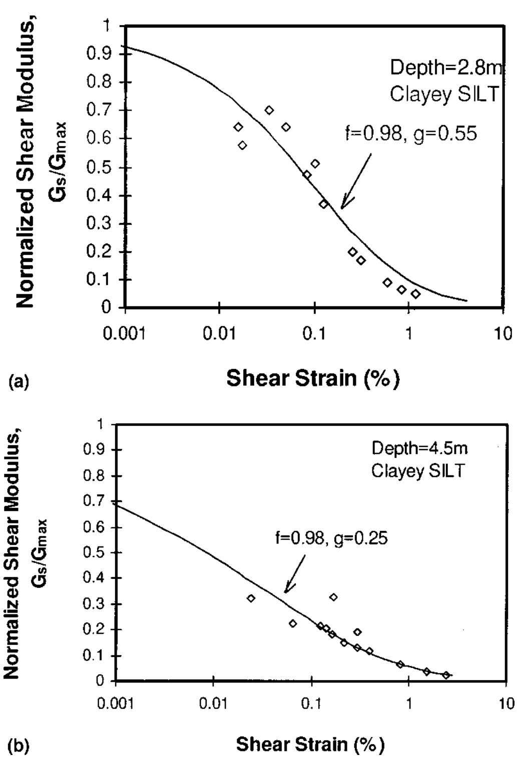

Fig. 16. Deduced $G_s/G_{\max}$-shear strain data and best fitting curve for Singapore pile

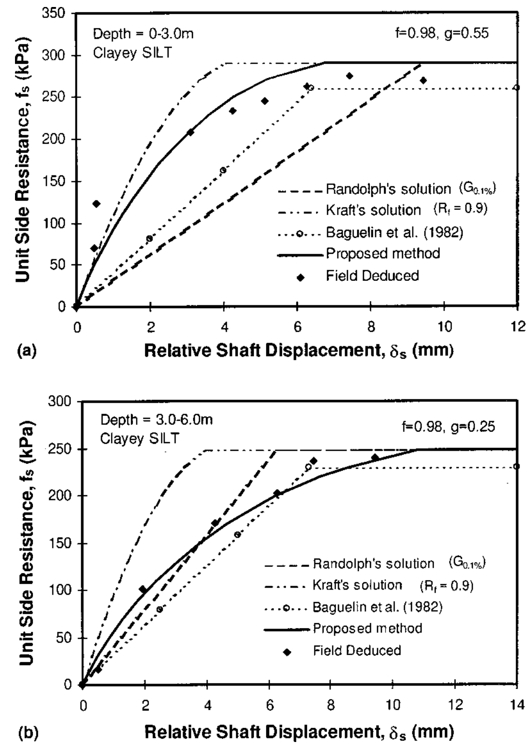

Fig. 17. Comparison of predicted and field deduced *t-z* curves for Singapore pile

two existing approximate analytical solutions and the empirical relationship proposed by Baguelin et al. (1982) is evident.

Due to insufficient load-transfer data for the lower geological strata, a complete load-displacement curve could not be produced for direct comparison with the corresponding field measured curve.

Conclusions

An analytical approach has been developed to account for the effect of the nonlinear decrease of the soil modulus with the strain/stress level on the load-transfer behavior along a bored pile. The modulus degradation curve, which is expressed as a modified hyperbola with two fitting parameters, can be evaluated from results of either a pile load test or a pressuremeter test. A procedure has been proposed to enable the fitting parameters to be determined from results of pressuremeter tests conducted in residual soils. Case studies of bored piles in two residual soils indicate that the nonlinear *t-z* curves and subsequently the load-displacement curves can be predicted using the proposed procedure with reasonable accuracy.

The proposed *t-z* curve is based on the theoretical framework developed by Randolph and Wroth (1978) and limitations inherent in the framework may exist in the present method.

Although some empirical correlations [e.g., Eqs. (12), (13), and (20)] suggested in this paper are relevant to the residual soil of Singapore, it is anticipated that the proposed model for generating the *t-z* curve from the PMT results is applicable to other soils as well.

Acknowledgments

The study on which this paper is based was supported by an applied research project funded by the Nanyang Technological

University, Singapore. The support provided by the university during the period of graduate study of the senior writer is gratefully appreciated. The writers also wish to thank Hock Lian Seng Engineering (Pte) Ltd. of Singapore for making the raw data from the Singapore test pile available.

Notation

The following symbols are used in this paper:

A = constant for estimating r_m;
A_g = constant for soil shear modulus distribution;
B = constant for estimating r_m;
c' = effective stress cohesion of soil;
d = diameter of shaft;
E_p = elastic modulus of pile;
E_{sL} = elastic modulus of soil at level of shaft base;
E_{sm} = elastic modulus of soil at middepth level;
f = constant for modified hyperbola;
f_k = factor reflecting construction effect on horizontal stress;
f_{su} = ultimate shaft resistance;
G = shear modulus of soil;
G_{ave} = average shear modulus of soil;
G_{max} = maximum shear modulus of soil;
G_p = pressuremeter shear modulus;
G_s = secant shear modulus;
G_{ur} = unload-reload pressuremeter shear modulus;
g = constant for modified hyperbola;
I_ρ = influence factor;
K = coefficient of earth pressure after pile installation;
K_0 = coefficient of earth pressure at rest;
k_t = tip stiffness;
L = pile length;
M_0 = modulus ratio of soil at shaft face;
N = standard penetration test (blows/300 mm);
n = power of shear modulus distribution;
p' = mean effective stress;
p_L = limit pressure;
p_L^* = net limit pressure;
Q = applied axial load at top of shaft;
Q_{ult} = ultimate shaft resistance;
q_t = tip resistance;
q_t^* = tip resistance corresponding to z_t^*;
R_f = failure ratio, empirical parameter in hyperbolic model;
r_m = maximum radius of influence zone;
r_0 = radius of shaft;
r_1 = radius of elastic-plastic boundary;
s_u = undrained shear strength;
z = depth below ground surface;
z_s = shaft displacement;
z_t = tip displacement;
z_t^* = maximum mobilized tip displacement in pile load test;
z_{tc} = critical tip displacement;
z_u = critical shaft displacement;
Δp = change in cavity pressure;
δ_s = relative displacement of pile shaft;
δ' = effective stress friction angle for soil-shaft interface;
ε_c = cavity strain;
ε_r = reference shear strain;
ε_s = shear strain;
ν_s = Poisson's ratio of soil;
ρ = inhomegeneity factor;
σ'_{h0} = initial effective horizontal stress;
σ'_{v0} = initial effective vertical stress;
τ_{max} = maximum shear stress;
τ_0 = shear stress on shaft surface; and
ϕ' = effective stress friction angle of soil.

References

Baguelin, F., Frank, R., and Jezequel, J. F. (1982). ''Parameters for friction piles in marine soils.'' *Proc., 2nd Int. Conf. in Numerical Methods for Offshore Piling*, ASCE, Austin, Tex., Vol. 2, 421–430.

Baguelin, F., Jezequel, J. F., and Shields, D. H. (1978). *The pressuremeter and foundation engineering*, Trans Tech, Clauthal, Germany.

Chang, M. F. (1988). ''In-situ testing of residual soils in Singapore.'' *Proc., 2nd Int. Conf. on Geomechanics in Tropical Soils*, ISSMFE, Singapore, Vol. 1, 97–108.

Chang, M. F., and Broms, B. B. (1991). ''Design of bored piles in residual soils based on field-performance data.'' *Can. Geotech. J.*, 28, 200–209.

Chang, M. F., and Goh, A. T. C. (1988). ''Behaviour of bored piles in residual soils and weathered rocks of Singapore.'' *Applied Research Rep.*, Nanyang Technological Institute, Singapore.

Chang, M. F., and H. Zhu (1998). ''A *t-z* curve with consideration of modulus degradation for pile analyses.'' *Proc., 13th Southeast Asian Geotechnical Conf.*, SEAGS, Taipei, Vol. 1, 461–466.

Colye, H. M., and Reese, L. C. (1966). ''Load transfer for axially loaded piles in clay.'' *J. Soil Mech. Found. Div.*, 92(2), 1–26.

Construction Industry Research and Information Association. (1985). ''Concrete pressure on formwork.'' *Rep. No. 108*, London.

de Moor, E. K. (1994). ''An analysis of bored pile/diaphragm wall installation effects.'' *Geotechnique*, 44(22), 341–347.

Fahey, M., and Carter, J. P. (1993). ''A finite element study of the pressuremeter test in sand using a nonlinear elastic plastic model.'' *Can. Geotech. J.*, 30, 348–362.

Ghionna, V. N., Karim, M., and Pedroni, M. (1994). ''Interpretation of unload-reload modulus from pressuremeter tests in sand.'' *Proc., 13th Int. Conf. on Soil Mechanics and Foundation Engineering*, ISSMFE, New Delhi, India, Vol. 1, 115–120.

Guo, W. D., and Randolph, M. F. (1997). ''Vertically loaded piles in non-homogeneous media.'' *Int. J. Numer. Analyt. Meth. Geomech.*, 21, 507–532.

Harris, E., and Mayne, P. (1994). ''Axial compression behavior of two drilled shafts in piedmont residual soils.'' *Proc., Int. Conf. on Design and Construction of Deep Foundation*, FWHA, Washington, D.C., Vol. 2, 352–367.

Jamiolkowski, M., Ladd, C., Germaine, J. T., and Lancellotta, R. (1985). ''New developments in laboratory and field testing of soils.'' *Proc., 11th Int. Conf. on Soil Mechanics and Foundation Engineering*, ISSMFE, San Francisco, Vol. 1, 57–153.

Jardine, R. J. (1991). ''Nonlinear stiffness parameters from undrained pressuremeter tests.'' *Can. Geotech. J.*, 29, 436–447.

Jardine, R. J., Potts, D. M., Fourie, A. B., and Burland, J. B. (1986). ''Studies of the influence of non-linear stress-strain characteristics in soil-structure interaction.'' *Geotechnique*, 36(3), 377–396.

Kondner, R. L. (1963). ''Hyperbolic stress-strain response: cohesive soils.'' *J. Soil Mech. Found. Div.*, 89(1), 115–143.

Kraft, L. M. J., Ray, R. P., and Kakaaki, T. (1981). ''Theoretical *t-z* curves.'' *J. Geotech. Eng. Div.*, 107(11), 1543–1561.

Kulhawy, F. H. (1984). ''Limiting tip and side resistance.'' *Proc., Symposium on Analysis and Design of Pile Foundation*, ASCE Convention, San Francisco, 80–98.

Kulhawy, F. H. (1991). ''Drilled shaft foundation.'' *Foundation engineering handbook*, 2nd Ed., H. Y. Fang, ed., Van Nostrand Reinhold, New York.

Lings, M. L., Ng, C. W. W., and Nash, D. F. T. (1994). ''The lateral pressure of wet concrete in diaphragm wall panels cast under bento-

nite.'' *Geotech. Eng.*, 107, 163–172.
Mair, R. J., and Wood, D. M. (1987). ''Pressuremeter testing: Methods and interpretation.'' *CIRIA Rep.*, Butterworths, London.
Mayne, P. W. (1995). ''Evaluation of foundation response by G/G_{max} degradation relationships in soils.'' National Science Council of ROC and NSF of U.S., Taipei, Taiwan, 136–148.
Mayne, P. W., and Kulhawy, F. H. (1982). ''K_0-OCR relationships in soil.'' *J. Geotech. Eng. Div.*, 108(6), 851–875.
Meyerhof, G. G. (1956). ''Penetration tests and bearing capacity of cohesionless soils.'' *J. Soil Mech. Found. Div.*, 82(1), 866–883.
O'Neill, M. W. (2001). ''Side resistance in piles and drilled shafts.'' *J. Geotech. Geoenviron. Eng.*, 127(1), 1–16.
Pinto, C. S., and Abramento, M. (1997). ''Pressuremeter tests on gneissic residual soil in Sao Paulo, Brazil.'' *Proc., 14th Int. Conf. on Soil Mechanics and Foundation Engineering*, ISSMFE, Hamburg, Germany, Vol. 1, 175–176.
Poulos, H. G., and Davis, E. H. (1980). *Pile foundation analysis and design*, Wiley, New York.
Powell, J. J. M., and Butcher, A. P. (1991). ''Assessment of ground stiffness from field and laboratory tests.'' *Associazione Geotechnica, Haliana*, Florence, Italy, Vol. 1, 153–156.
Rahardjo, H., Lim, T. T., Chang, M. F., and Fredlund, D. G. (1995). ''Shear strain characteristics of a residual soil.'' *Can. Geotech. J.*, 32(1), 60–77.
Randolph, M. F., and Wroth, C. P. (1978). ''Analysis of deformation of vertically loaded piles.'' *J. Geotech. Eng. Div.*, 104(12), 1465–1488.
Randolph, M. F., and Wroth, C. P. (1979). ''A simple approach to pile design and the evaluation of pile tests.'' *Behavior of deep foundation, STP 670*, ASTM, Philadelphia, 484–499.
Reese, L. C., and O'Neill, M. W. (1988). ''Drilled shafts: construction procedures and design methods.'' *Rep. No. FHWA-HI-88-042*, Federal Highway Administration, McLean, Va.
Vijayvergiya, V. N. (1977). ''Load-movement characteristic of piles.'' *Proc., Port'77*, ASCE, New York, 269–284.
Withiam, J. L., and Kulhawy, F. H. (1981). ''Analysis procedure for drilled shaft uplift capacity.'' *Proc., ASCE Convention*, St. Louis, 82–97.
Yong, R. N., Chen, C. K., Sellappah, J., and Chong, T. S. (1985). ''The characterization of residual soils in Singapore.'' *Proc., 8th Southeast Asian Geotechnical Conf.*, Kuala-Lumpur, Malaysia, Vol. 1, 3-19–3-26.
Zhu, H. (2000). ''Evaluation of load transfer behavior of bored piles in residual soil incorporating construction effect.'' PhD thesis, Nanyang Technological Univ., Singapore.

J. Geotech. Geoenviron. Eng. 2002.128:764-774.